Contribution from the Fakultät für Chemie der Universität Bielefeld, Postfach 86 40, D-4800 Bielefeld 1, FRG, and Anorganisch-Chemisches Institut der Universität Bonn, Gerhard-Domagk-Strasse 1, D-5300 Bonn 1, FRG

Unusual Bonding in a Main-Group Multiple-Bonded System: Umbrella-Shaped Diphosphenes†

T. Busch,‡ W. W. Schoeller,*,‡ E. Niecke,*,§ M. Nieger,§ and H. Westermann§

Received November 17, 1988

Quantum-chemical calculations at an ab initio double-ζ level predict an unusual bonding situation for diphosphenes that are substituted by an electronegative group (atom). The latter withdraws electron density from the neighboring phosphorus atom, so as to promote the close ion pair X^-PPH^+. The PPH^+ fragment is bridged rather than linear. It is isoelectronic with Si_2H_2, which also possesses a bridged structure. Consequently, depending on the substituents, diphosphenes can adopt an umbrella conformation with a valence angle at the double-bonded phosphorus smaller than 90°. The theoretical concept is explored by calculation of typical model compounds and is verified by a selected variety of synthesized and structurally characterized new type of diaminophosphino-substituted diphosphenes. The coupling constant between the 1,3-positioned phosphorus atoms varies from 400 to 600 Hz.

Introduction

Within this decade a great deal of effort has been dedicated to the evaluation of bonding between heavier main-group elements,[1] including even stable metal-metal double bonds such as in digermenes.[1d] Hitherto these new systems have mainly been characterized by spectroscopic and reactive studies; structural investigations are rare so far. For the case of the phosphorus-phosphorus double bonds structures of symmetrically (**1**, $R^\alpha = R^\beta$; Chart I) as well as unsymmetrically substituted systems are known. All these systems indicate a trans rather than cis conformation of the substituents.[2] In the case of a symmetrical substitution the PP double-bond distance is 203 pm and the valence angle PPR is approximately 100-110°, depending on the substituents.

In the present publication we explore unusual bonding features of substituted diphosphenes, for the case of the substituents differing considerably in electronegativity. It will be shown that if R^α is a strong electronegative group (atom), e.g., NH_2, OH, and Hal, compared to R^β, the valence angle $P^\alpha P^\beta R^\beta$ is decreased, resulting in the adoption of an umbrella conformation at P^β, while at the same time the angle at P^α is increased. In the second part of our publication the theoretical model is supported by a selected variety of substituted diphosphenes, synthesized and structurally characterized for this purpose.

Theoretical Section

The quantum-chemical investigations are based on the results of ab initio calculations at a double-ζ level. The following basis sets were constructed from Huzinaga bases:[3] C, N, O, F (8s, 4p) in the contraction [5, 3×1/3, 1] + 1d (0.8, 0.95, 1.25, 1.40 for C, N, O, F]; P, Si (10s, 6p) in the contraction [4, 6×1/3, 3×1] + 1d (0.5, 0.40 for P, Si]; H (4s) in contraction [3, 1]. The electronic hypersurface of P_2H^+ was calculated with an extended basis set: P [5, 6×1/4, 3×1/d_1 = 0.8, d_2 = 0.25]; H [3, 1/p_1 = 1.20, p_2 = 0.30]. All SCF calculations were performed with the Karlsruhe version of the Columbus set of programs.[4] The energy optimization of the structures was performed with the Mutargh-Sargent algorithm.[5] All energy minima are obtained with an accuracy of 10^{-9} au. Thus, we obtained the bond lengths (bond angles) with an accuracy of 0.1 pm (0.05°).

In the case of P_2H_2, FP_2H, and P_2H^+ additional CI calculations at the CEPA-1 level with the self-consistent electron-pair (SCEP) method[6a] were performed. The structures of FP_2H and P_2H^+ were also optimized by means of a MCSCF gradient technique.[6b] All correlation calculations were carried out with the program system MOLPRO-88.[6]

Experimental Section

The syntheses of the various unsymmetrically substituted diphosphenes were performed according to Scheme I. The dichlorodiphosphane **2** was reacted with the lithium phosphide **3**; $ClSiMe_3$ was eliminated via the intermediate **4**. Alternatively the disilyldiphosphane **5** was allowed to react with the dichlorophosphanes **6b-g**. All diphosphenes are stable at room temperature with respect to dimerization to **9**, except **8b**, which reacted at room temperature within a few hours by (2 + 2) cycloaddition to result in **9b**.[22] In detail, the individual compounds were obtained by the following procedures. $(^iPr_2N)_2PPCl_2$ (**2**),[7] Mes*(PLi)$SiMe_3$ (**3**),[8] $(^iPr_2N)_2PP(SiMe_3)_2$ (**5**),[7] $(Me_3Si)_2N(Me_3Si)NPCl_2$ (**6c**),[9] $^iPr_2NPCl_2$ (**6b**),[10] (TMP)PCl_2 (**6d**)[10] (TMP = 2,2,6,6-tetramethylpiperidino), Mes*N(H)PCl_2 (**6e**)[11] (Mes* = 2,4,6-tri-*tert*-butylphenyl), $(Me_2Bu^t_2Si)_2NPCl_2$ (**6f**),[11] and Mes*$OPCl_2$ (**6g**)[12] were prepared as described in the literature.

Chart I

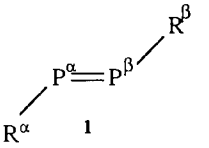

Preparation of $(^iPr_2N)_2P(P)PMes^*$ (8a). A stirred solution of 1.66 g (5 mmol) of $(^iPr_2N)_2PPCl_2$ in 20 mL of diethyl ether was cooled to -68 °C, and 1.78 g (5 mmol) of Mes*P(Li)$SiMe_3$, dissolved in 10 mL of diethyl ether, was added via a syringe. The solution was allowed to warm slowly to -20 °C, where ^{31}P NMR spectroscopy shows the formation of the intermediate $(^iPr_2N)_2PP(Cl)P(SiMe_3)Mes^*$.[13] After the mixture

† Presented at the EUCHEM conference PSIBLOC in Paris, France, Aug 1988.

‡ Universität Bielefeld.

§ Universität Bonn.

(1) (a) Cowley, A. H. *Polyhedron* **1984**, *3*, 389. (b) Raabe, G.; Michl, J. *Chem. Rev.* **1985**, *85*, 419. (c) West, R. *Angew. Chem.* **1987**, *99*, 1231. (d) Goldberg, D. E.; Harris, D. H.; Lappert, M. F.; Thomas, K. M. *J. Chem. Soc., Chem. Commun.* **1976**, 261. Goldberg, D. E.; Hitchcock, P. B.; Lappert, M. F.; Thomas, K. M.; Thorne, A. J.; Fjeldberg, T.; Haaland, A.; Schilling, B. E. R. *J. Chem. Soc., Dalton Trans.* **1986**, 2387.

(2) (a) Yoshifuji, M.; Shima, I.; Inamoto, N. *J. Am. Chem. Soc.* **1981**, *103*, 4587. (b) Cowley, A. H.; Kilduff, J. E.; Norman, N. C.; Pakulski, M.; Altwood, J. L.; Hunter, W. E. *J. Am. Chem. Soc.* **1983**, *105*, 4845. (c) Niecke, E.; Rüger, R.; Lysek, M.; Pohl, S.; Schoeller, W. W. *Angew. Chem.* **1983**, *95*, 495. (d) Jaud, J.; Couret, C.; Escudie, J. *J. Organomet. Chem.* **1983**, *249*, 25. (e) Jutzi, P.; Meyer, U.; Krebs, B.; Dartmann, M. *Angew. Chem.* **1986**, *98*, 894. (f) Weber, L.; Reizig, K.; Bungardt, D.; Boese, R. *Organometallics* **1987**, 110.

(3) Huzinaga, S. "Approximate Atomic Functions. II"; Technical Report; The University of Alberta: Edmonton, Alberta, Canada, 1971.

(4) Ahlrichs, R.; Böhm, H. J.; Ehrhardt, C.; Scharf, P.; Schiffer, H.; Lischka, H.; Schindler, M. *J. Comput. Chem.* **1985**, *6*, 200.

(5) The computer program for energy optimization of structures was written by one of us (Busch, T. Unpublished results).

(6) MOLPRO-88 is the MOLPRO version by H. J. Werner and P. J. Knowles. (a) Meyer, W. *J. Chem. Phys.* **1973**, *58*, 1017. Werner, H. J.; Reinsch, E. A. *J. Chem. Phys.* **1982**, *76*, 3144. (b) Werner, H. J.; Meyer, W. *J. Chem. Phys.* **1980**, *73*, 2342. Werner, H. J.; Knowles, P. J. *J. Chem. Phys.* **1985**, *82*, 5053. Pulay, P. *J. Chem. Phys.* **1983**, *78*, 5043.

(7) Niecke, E.; Westermann, H.; Nieger, M. To be submitted for publication in *Z. Naturforsch.*

(8) $^tBu_3C_6H_2P(SiMe_3)Li$ was prepared in analogy to the method for $^tBu_3C_6H_2P(SiMe_2^tBu)Li$; see: Yoshifuji, M.; Toyota, K.; Shibayama, K.; Inamoto, N. *Chem. Lett.* **1983**, 1653.

(9) Niecke, E.; Altmeyer, O.; Nieger, M.; Knoll, F. *Angew. Chem., Int. Ed. Engl.* **1987**, *26*, 12.

(10) King, R. B.; Sadanani, N. D. *Synth. React. Inorg. Met.-Org. Chem.* **1985**, *15*, 149.

(11) Lysek, M. Doctoral thesis, Bielefeld, FRG, 1988.

(12) Flynn, K. M.; Bartlett, R. A.; Olmstead, M. M.; Power, P. P. *Organometallics* **1986**, *5*, 813.

0020-1669/89/1328-4334$01.50/0

Scheme I

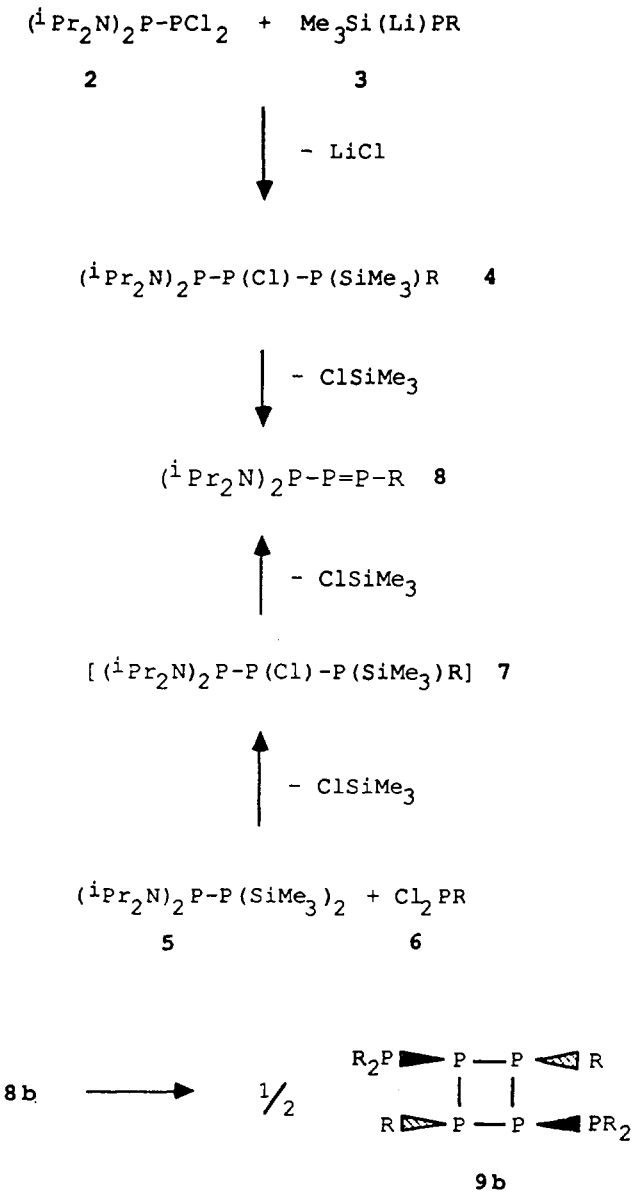

3, 4, 8: R = Mes* (**a**)
6–9: R = $^{i}Pr_2N$ (**b**)
6–8: R = $Me_3Si(Me_3Si_2N)N$ (**c**), $(-Me_2C(CH_2)_3CMe_2-)N$ (**d**), Mes*NH (**e**), $(Me_2Bu^{t}Si)_2N$ (**f**), Mes*O (**g**)

was stirred overnight at ambient temperature the ^{31}P NMR spectrum showed complete conversion to $(^{i}Pr_2N)_2P(P)PMes^*$. The solvent and all volatile materials were removed in vacuo, and the oily residue was dissolved in a small amount of diethyl ether. Cooling the solution to −80 °C gave 0.84 g (31% yield) of dark red crystalline $(^{i}Pr_2N)_2P(P)$-$PC_6H_2{}^{t}Bu_3$, mp 110–112 °C. Anal. Calcd for $C_{30}H_{57}N_2P_3$: C, 66.94; H, 10.59; N, 5.20. Found: C, 66.05; H, 9.73; N, 4.97.

Preparation of $(^{i}Pr_2N)_2P(P)PN^{i}Pr_2$ (8b). A solution of 2.04 g (5 mmol) of $(^{i}Pr_2N)_2PP(SiMe_3)_2$ and 1.01 g (5 mmol) of $^{i}Pr_2NPCl_2$ in 25 mL of diethyl ether was stirred at −4 °C in the presence of a catalytic amount of $(Me_2N)_3P(O)$. The reaction was monitored by ^{31}p NMR spectroscopy. After completion of the reaction the solution was filtered and all volatile materials were removed under vacuum at −15 °C to give 1.73 g (88% yield) of crude intense orange oily $(^{i}Pr_2N)_2P(P)PN^{i}Pr_2$, which dimerizes on standing at 25 °C within a few hours. Dissolution of the resulting tetraphosphetane in a small amount of diethyl ether and crystallization at −30 °C gave 0.56 g (14% yield) of light yellow crystalline $[(^{i}Pr_2N)_2PPP(N^{i}Pr_2)]_2$ (**9b**), mp 192–195 °C. Anal. Calcd for $C_{36}H_{84}N_6P_6$: C, 54.99; H, 10.68; N, 10.69. Found: C, 55.46; H, 11.46; N, 10.87. Mass spectrum (selection) (*m/e* (relative intensities)): 455 (1), 355 (5), 324 (3), 293 (1), 262 (6), 231 (21), 132 (100), 124 (60).

(13) $^{31}P\{^{1}H\}$ data: 131.5, 73.6, −67.0 ppm (J_{PP} = 546, 296, 142 Hz).

The ^{31}P NMR spectrum shows two complex multiplets centered at 77 ppm $[(^{i}Pr_2N)_2P-]$ and −11 ppm (ring P).

Preparation of $(^{i}Pr_2N)_2P(P)PN(SiMe_3)N(SiMe_3)_2$ (8c). A stirred solution of 1.46 g (3.58 mmol) of $(^{i}Pr_2N)_2PP(SiMe_3)_2$ in 25 mL of diethyl ether was cooled to −15 °C, and 2.4 mL of *n*-butyllithium (1.6 M in hexane) was added via a syringe. The solution was brought to ambient temperature and stirred overnight. ^{31}P NMR spectroscopy shows the complete conversion to $(^{i}Pr_2N)_2PP(Li)SiMe_3$ ($\delta(^{31}P)$: 85.7, −197.6 ($^{1}J_{PP}$ = 312 Hz)). The reaction mixture was now cooled to −68 °C, and a solution of 1.25 g (3.58 mmol) of $(Me_3Si)_2N(SiMe_3)NPCl_2$ in 5 mL of diethyl ether was added. The solution was then stirred at ambient temperature for 2 days. Filtration and subsequent removal of all volatile materials in vacuo left 1.57 g (81% yield) of an orange oil. Anal. Calcd for $C_{21}H_{55}N_4P_3Si_3$: C, 46.67; H, 10.18; N, 10.37. Found: C, 44.38; H, 9.60; N, 10.93.

Preparation of $(^{i}Pr_2N)P(P)P(TMP)$ (8d). A solution of 2.04 g (5 mmol) of $(^{i}Pr_2N)_2PP(SiMe_3)_2$ and 1.21 g (5 mmol) of $(TMP)PCl_2$ in 25 mL of diethyl ether containing several drops of $(Me_2N)_3P(O)$ was stirred at 15 °C. The reaction was monitored by ^{31}P NMR spectroscopy. After completion of the reaction, the solvent and all volatile materials were removed in vacuo. The oily residue was dissolved in a small amount of 1:1 diethyl ether/pentane. Cooling the solution to −30 °C gave 0.47 g (22% yield) of orange crystalline $(^{i}Pr_2N)_2P(P)P(TMP)$, mp 80–82 °C. Anal. Calcd for $C_{21}H_{46}N_3P_3$: C, 58.33; H, 10.62; N, 9.70. Found: C, 57.66; H, 9.29; N, 9.31.

Preparation of $(^{i}Pr_2N)_2P(P)PN(H)Mes^*$ (8e). A solution of 2.04 g (5 mmol) of $(^{i}Pr_2N)_2PP(SiMe_3)_2$ and 1.91 g (5 mmol) of $Mes^*N(H)PCl_2$ in 30 mL of 1:1 diethyl ether/THF containing a catalytic amount of $(Me_2N)_3P(O)$ was stirred for 3 days at ambient temperature. Evaporation of all volatile materials left 2.6 g (94% yield) of crude, dark red, oily $(^{i}Pr_2N)_2P(P)PN(H)Mes^*$. Anal. Calcd for $C_{30}H_{58}N_3P_3$: C, 65.13; H, 10.48; N, 7.59. Found: C, 62.78; H, 8.14; N, 7.43.

Preparation of $(^{i}Pr_2N)_2P(P)PN(SiMe_2{}^{t}Bu)_2$ (8f). A solution of 2.04 g (5 mmol) of $(^{i}Pr_2N)_2PP(SiMe_3)_2$ and 1.73 g (5 mmol) of $(^{t}BuMe_2Si)_2NPCl_2$ in 30 mL of THF containing a few drops of $(Me_2N)_3P(O)$ was stirred at ambient temperature for 5 days. After removal of the solvent and all volatile materials under vacuum the residue was dissolved in a small amount of THF. Cooling the solution to −80°C gave 0.29 g (11% yield) of orange crystalline $(^{i}Pr_2N)_2P(P)PN$-$(SiMe_2{}^{t}Bu)_2$, mp 90–93 °C. Anal. Calcd for $C_{24}H_{58}N_3P_3Si_2$: C, 53.64; H, 10.79; N, 7.82. Found: C, 52.39; H, 9.98; N, 7.05.

Preparation of $(^{i}Pr_2N)_2P(P)POMes^*$ (8g). A solution of 2.04 g (5 mmol) of $(^{i}Pr_2N)_2PP(SiMe_3)_2$ and 1.81 g (5 mmol) of Mes^*OPCl_2 in 30 mL of 2:1 ethylether/THF containing a catalytic amount of $(Me_2N)_3P$-(O) was stirred at ambient temperature for 3 days. After the solvent and all volatile materials were removed in vacuo, the oily residue was dissolved in THF. Cooling the solution of −35 °C gave 1.09 g (39% yield) of deep orange crystalline $(^{i}Pr_2N)_2P(P)POMes^*$. Anal. Calcd for $C_{30}H_{57}N_2OP_3$: C, 65.01, H, 10.28; N, 5.05. Found: C, 63.68; H, 9.34; N, 4.40.

All manipulations were carried out under dry oxygen-free conditions by using vacuum-line or Schlenk techniques. Hydrocarbon solvents, diethyl ether, and THF were refluxed over sodium benzophenone ketyl and dichloromethane and acetonitrile over CaH_2 and prior to use were distilled under N_2.

Melting point determinations were carried out in sealed tubes and are uncorrected.

Microanalyses were performed by Beller, Göttingen, FRG, or on a Heraeus CHN-O-Rapid instrument.

X-ray Crystallographic Studies of 8d, 8f, and 8a. All X-ray data were collected with a Nicolet R3m diffractometer at room temperature. Calculations were carried out on a Data General NOVA-3 computer using the SHELTXL programs, version 4 [Sheldrick, G. M. *SHELXTL. An Integrated System for Solving, Refining and Displaying Crystal Structures from Diffraction Data*, University of Göttingen, 1978. Sheldrick, G. M. *SHELXTL User Manual*; Nicolet XRD Corp.: Freemont, CA, 1981]. The structures were solved by direct methods. All non-hydrogen atoms were refined anisotropically. H atoms located by difference electron density determination and refined by using a riding model (isotropic thermal parameters were fixed at 1.2 times that of the bonded carbon, and the C–H distance was fixed at 0.96 Å). Further details are given in Table I. The atomic coordinates and isotropic temperature factors are given in Tables II–IV.

Results and Discussion

a. Model Geometries. We begin our discussion with an analysis of bonding in model geometries of substituted diphosphenes, calculated at an ab initio single-determinant SCF level. The various energy-optimized structures are shown in Figure 1. The corresponding total energies (in au) are given in Table V.

Table I. Crystallographic Data and Summary of Data Collection and Refinement[a]

	8d	**8f**	**8a**
formula	$C_{21}H_{46}N_3P_3$	$C_{24}H_{58}N_3P_3Si_2$	$C_{30}H_{57}N_2P_3$
cryst syst	monoclinic	monoclinic	monoclinic
space group	$P2_1/c$ (No. 14)	$P2_1/c$ (No. 14)	$P\bar{1}$ (No. 2)
a, Å	13.130 (4)	13.345 (4)	10.208 (2)
b, Å	11.170 (5)	18.808 (8)	13.635 (4)
c, Å	18.764 (7)	14.753 (3)	14.323 (4)
α, deg			68.61 (2)
β, deg	94.96 (3)	111.80 (2)	75.43 (2)
γ, deg			68.24 (2)
V, Å^3	2742	3438	1708
Z	4	4	2
ρ_{calc}, g cm^{-3}	1.05	1.04	1.05
μ, mm^{-1}	0.22	0.25	0.19
max 2θ, deg	50	50	50
no. of unique obsd data ($\|F\| > 4\sigma(F)$)	2503	4023	4863
no. of variables	244	289	316
R	0.068	0.053	0.051
R_w	0.061	0.052	0.055

[a] All data were taken with Mo Kα radiation with λ = 0.71069 Å by using the ω-scan technique. $R = \sum||F_o| - |F_c||/\sum|F_o|$ and $R_w = \sum(|F_o| - |F_c|)w^{1/2}/\sum|F_o|w^{1/2}$ with the weighting scheme $w^{-1} = \sigma^2(F) + 0.0005F^2$.

Table II. Atom Coordinates (×10^4) and Temperature Factors (Å^2 × 10^3) for **8a**

	x	y	z	U[a]
P(1)	2799 (1)	3465 (1)	2985 (1)	46 (1)
P(2)	3503 (1)	2012 (1)	4056 (1)	48 (1)
P(3)	2188 (1)	2714 (1)	5309 (1)	43 (1)
C(11)	3886 (2)	3138 (2)	1820 (2)	38 (1)
C(12)	5278 (2)	3220 (2)	1539 (2)	41 (1)
C(13)	6185 (2)	2702 (2)	841 (2)	50 (1)
C(14)	5791 (3)	2169 (2)	362 (2)	51 (1)
C(15)	4377 (3)	2227 (2)	557 (2)	50 (1)
C(16)	3393 (2)	2714 (2)	1255 (2)	42 (1)
C(40)	5896 (3)	3874 (2)	1915 (2)	53 (1)
C(41)	6740 (4)	4515 (3)	1016 (3)	93 (2)
C(42)	6888 (4)	3076 (3)	2681 (2)	90 (2)
C(43)	4800 (4)	4754 (3)	2358 (4)	113 (3)
C(50)	6840 (3)	1585 (3)	−386 (2)	69 (1)
C(51)	6340 (4)	2029 (4)	−1389 (2)	115 (2)
C(52)	7096 (7)	380 (4)	23 (3)	183 (3)
C(53)	8306 (4)	1748 (6)	−557 (4)	191 (5)
C(60)	1814 (3)	2788 (2)	1344 (2)	53 (1)
C(61)	1490 (3)	2768 (3)	354 (2)	86 (2)
C(62)	794 (3)	3882 (3)	1492 (3)	83 (2)
C(63)	1473 (3)	1812 (3)	2194 (3)	82 (2)
N(2)	1030 (2)	1981 (2)	5861 (2)	52 (1)
C(21)	1426 (3)	765 (2)	6253 (2)	57 (1)
C(22)	945 (4)	260 (3)	5672 (3)	90 (2)
C(23)	876 (4)	382 (3)	7375 (2)	84 (2)
C(24)	−513 (3)	2589 (3)	5795 (2)	70 (1)
C(25)	−1071 (4)	3503 (3)	6275 (3)	99 (2)
C(26)	−851 (4)	3009 (4)	4707 (3)	100 (2)
N(3)	3469 (2)	2265 (2)	6056 (2)	54 (1)
C(31)	4626 (3)	1200 (2)	6233 (2)	62 (1)
C(32)	4538 (4)	483 (3)	7328 (2)	85 (2)
C(33)	6080 (3)	1331 (4)	5869 (3)	104 (2)
C(34)	3504 (4)	3040 (3)	6538 (2)	83 (2)
C(35)	3895 (6)	4038 (3)	5746 (3)	134 (3)
C(36)	2178 (5)	3357 (4)	7236 (4)	144 (3)

[a] Equivalent isotropic U defined as one-third of the trace of the orthogonalized U_{ij} tensor.

Let us first consider the parent compound **1** ($R^\alpha = R^\beta = H$) of the diphosphene series. The valence angle HPP is 95.2°. It is slightly larger (100.4°) in the cis conformation. The resulting PP double-bond length is for both structures about 200 pm, in good agreement with 203 pm observed from the previously known experimental structures of symmetrically substituted diphosphenes.[2] As one expects, the trans conformation is slightly more stable than the cis conformation. Inclusion of electron correlation in the wave function (at the CEPA-1 level with all double excitations from the valence orbitals) does not considerably affect this energy difference. Consequently, we have not studied the effect of electron correlation on the whole series of di-

Table III. Atom Coordinates (×10^4) and Temperature Factors (Å^2 × 10^3) for **8d**

	x	y	z	U[a]
P(1)	274 (1)	7051 (1)	1011 (1)	58 (1)
P(2)	1289 (1)	8098 (1)	1602 (1)	66 (1)
P(3)	2436 (1)	7759 (1)	813 (1)	52 (1)
N(1)	−861 (3)	6865 (3)	1358 (2)	55 (1)
C(11)	−1165 (3)	7446 (4)	2037 (3)	59 (2)
C(12)	−2306 (4)	7262 (5)	2126 (3)	100 (3)
C(13)	−2698 (4)	6040 (6)	1991 (4)	103 (3)
C(14)	−2525 (4)	5730 (6)	1225 (4)	114 (3)
C(15)	−1419 (4)	5778 (4)	1052 (3)	65 (2)
C(16)	−1419 (4)	5731 (6)	241 (3)	107 (3)
C(17)	−864 (4)	4656 (5)	1356 (3)	108 (3)
C(18)	−525 (4)	6937 (5)	2690 (3)	79 (2)
C(19)	−1025 (4)	8794 (4)	1992 (3)	82 (2)
N(2)	3502 (3)	7489 (3)	1379 (2)	60 (1)
C(21)	3919 (4)	8352 (5)	1923 (3)	74 (2)
C(22)	5001 (4)	8700 (7)	1801 (4)	121 (3)
C(23)	3849 (5)	7929 (6)	2690 (3)	109 (3)
C(24)	3922 (4)	6275 (5)	1405 (3)	83 (2)
C(25)	4361 (5)	5918 (6)	720 (4)	134 (3)
C(26)	3179 (4)	5331 (5)	1624 (4)	121 (3)
N(3)	2559 (3)	9131 (4)	452 (2)	59 (2)
C(31)	2340 (4)	10284 (4)	781 (3)	66 (2)
C(32)	1336 (4)	10835 (5)	453 (3)	97 (3)
C(33)	3215 (4)	11169 (5)	785 (3)	104 (3)
C(34)	2721 (4)	9180 (5)	−322 (3)	76 (2)
C(35)	3767 (5)	8729 (7)	−457 (3)	133 (4)
C(36)	1907 (4)	8538 (5)	−782 (3)	101 (3)

[a] Equivalent isotropic U defined as one-third of the trace of the orthogonalized U_{ij} tensor.

Table IV. Atom Coordinates (×10^4) and Temperature Factors (Å^2 × 10^3) for **8f**

	x	y	z	U[a]
P(1)	3520 (1)	3144 (1)	2557 (1)	50 (1)
P(2)	4120 (1)	3378 (1)	1528 (1)	58 (1)
P(3)	5787 (1)	3226 (1)	2621 (1)	43 (1)
N(1)	2121 (2)	3179 (1)	2074 (2)	45 (1)
Si(1)	1452 (1)	3977 (1)	1574 (1)	52 (1)
C(1)	−30 (3)	3846 (2)	960 (4)	97 (2)
C(2)	1891 (4)	4352 (3)	607 (3)	100 (2)
C(3)	1686 (3)	4666 (2)	2565 (3)	67 (2)
C(4)	1053 (4)	5343 (2)	2119 (4)	107 (3)
C(5)	1312 (4)	4391 (3)	3361 (3)	115 (3)
C(6)	2877 (3)	4870 (2)	3048 (4)	106 (3)
Si(2)	1559 (1)	2378 (1)	2295 (1)	53 (1)
C(7)	2505 (4)	1970 (2)	3453 (3)	94 (2)
C(8)	256 (3)	2503 (3)	2479 (4)	93 (2)
C(9)	1326 (3)	1734 (2)	1253 (3)	61 (2)
C(10)	778 (4)	1060 (2)	1417 (4)	102 (3)
C(11)	604 (4)	2057 (3)	281 (3)	102 (2)
C(12)	2394 (3)	1523 (2)	1172 (3)	91 (2)
N(2)	6382 (2)	3985 (1)	2473 (2)	51 (1)
C(21)	6275 (4)	4319 (2)	1538 (3)	79 (2)
C(22)	5669 (4)	5021 (2)	1377 (3)	116 (3)
C(23)	7356 (5)	4391 (3)	1430 (4)	151 (4)
C(24)	6925 (3)	4423 (2)	3350 (3)	69 (2)
C(25)	6164 (4)	4668 (3)	3837 (3)	112 (3)
C(26)	7915 (4)	4074 (3)	4067 (4)	142 (3)
N(3)	6192 (2)	2535 (1)	2112 (2)	49 (1)
C(31)	6677 (3)	1926 (2)	2745 (3)	65 (2)
C(32)	5936 (4)	1585 (2)	3179 (4)	98 (3)
C(33)	7766 (3)	2111 (2)	3532 (3)	91 (2)
C(34)	5967 (3)	2432 (2)	1066 (3)	73 (2)
C(35)	5175 (4)	1822 (2)	625 (3)	102 (2)
C(36)	6995 (4)	2331 (3)	867 (3)	112 (3)

[a] Equivalent isotropic U defined as one-third of the trace of the orthogonalized U_{ij} tensor.

Table V. Energies of Trans (First Entry) and Cis (Second Entry) Isomers of Monosubstituted Diphosphenes **1** (R^β = H)

R^α	E, au[a]	ΔE, kcal/mol[b] SCF	CEPA-1
H	−682.440 322	0.0	0.0
	−682.434 026	3.95	3.80
F	−781.305 211	0.0	0.0
	−781.301 638	2.24	1.81
Cl	−1141.284 136	0.0	0.0
	−1141.279 592	2.85	
OH	−751.299 615	0.0	
	−751.296 215	2.13	
NH_2	−731.475 590	0.0	
	−731.471 412	2.62	
CH_3	−721.471 605	0.0	
	−721.465 554	3.80	
SiH_3	−912.457 435	0.0	
	−912.450 926	4.08	

[a] SCF energies. [b] E(cis) − E(trans).

Chart II

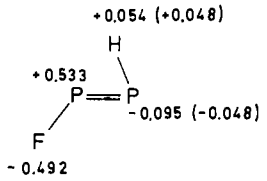

phosphenes. Our results on the parent diphosphene are also in good agreement with the results of Boggs et al.[14]

Next we will consider the effect of substituents on the structure of the diphosphene. For this purpose we have examined a variety of model compounds (Figure 1 and Table V). Surprisingly, with increasing electronegativity of the ligand R^α the parent structure changes considerably. Most noticeable is the change of the HPP valence angle at P^β. The angle is decreased, such as to become even smaller than 90° (for the trans conformation). Concomitantly the valence angle at P^α does the opposite; it is slightly increased. It is of interest to note that these effects are exerted in the trans and in the cis conformations.

In order to account for the influence of electron correlation, we optimized the structure of *trans*-FP_2H at the MCSCF level. The active space in the calculation included all virtual orbitals, which are expected from the valence space. This leads to the consideration of 19a′ and 5a″ orbitals within C_s symmetry (SCF: 16a′, 4a″). The MO's up to 13a′ and 2a″ were regarded as doubly occupied in all configuration state functions (CSF's) in order to limit the configuration space. The optimized geometry parameters (R_{PP} = 2.072 Å, R_{PH} = 1.459 Å, R_{PF} = 1.602 Å, ∠PPH = 86.10°, ∠PPF = 102.55°) indicate that the small PPH angle is not an artifact of the SCF calculation; it is even slightly decreased in the MCSCF case.

A more detailed insight into bonding is given by a Mulliken population analysis.[15] We will investigate it at FPPH in its trans conformation, which reveals the most pronounced effect in the valence angle decrease at P^β (Chart II). Compared to phosphorus the fluorine is considerably more electronegative.[16] Consequently it withdraws electron density mainly from its neighboring atom. According to the Mulliken population analysis the atom P^α donates almost 0.5 electron to its neighboring fluorine atom. For comparison the values for the Mulliken population analysis for the parent **1** (R^α = R^β = H, trans conformation) are added in parentheses. On this basis the PF bond is very polar and the bonding situation may be accounted for by a strong contribution of the canonical structure shown in Scheme II. An anion (fragment A) forms a strong ionic bond with the cation (fragment B). With regard to the overlap population between H and P^α, the Mulliken population analysis gives only a small antibonding overall contribution of −0.063 (*trans*-P_2H_2 −0.087). This leads to the conclusion that we have in the case of FP_2H an umbrella-shaped structure with no real bridged bond. This view is also supported by an analysis of the electron distributions in both structures (not recorded here).

Scheme II

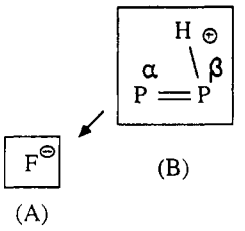

Chart III

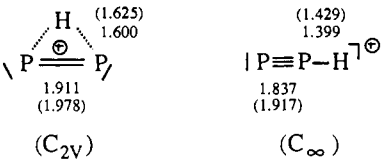

Table VI. Absolute Energies (in au) for P_2H^+

structure	SCF	CEPA-1[a]	MCSCF[b]	CEPA-1[b]
cyclic	−681.676 25	−681.941 41	−681.770 83	−682.166 44
linear	−681.649 68	−681.921 23	−681.768 04	−682.147 04

[a] Optimized at SCF level. [b] Optimized at MCSCF level.

b. Bridging in P_2H^+. As is obtained by the numerical calculations the decrease of the valence angle P^β parallels the ionic character of the $P^\alpha R^\alpha$ bond. Therefore, it seems logical to analyze the electronic hypersurface of P_2H^+. It was investigated at the SCF and CEPA-1 level (with the extended basis set; see Theoretical Section). The potential surface of P_2H^+ as a function of the valence angle HPP is recorded in Figure 2.

Each point of the hypersurface is obtained by energy optimization at the SCF level (at times for fixed HPP angles). The CEPA-1 calculations were carried out at these geometries. A cyclic structure appears to be a minimum while the linear form can be regarded as a saddle point. The flattening of the potential curve at 90° is due to the influence of a low-lying antibonding a′ orbital, which contributes most strongly to the correlation energy.

In order to examine further the influence of electron correlation, we performed in addition a geometry optimization at the MCSCF level using the extended basis set. The active space was chosen to be identical with the valence space. The core orbitals were regarded as closed and did not participate in the construction of the CSF's. Hence, this led to a configuration space of about 1400 CSF's. The resulting geometrical parameters (SCF level, MCSCF values in parentheses) are as shown in Chart III. Corresponding energy values are given in Table VI. At all levels a bridged structure is favored (SCF, 16.7 kcal/mol; MCSCF, 5.7 kcal/mol; CEPA-1, 12.2 kcal/mol). The small energy difference between cyclic and linear structures indicates an easily feasible migration of the H atom in P_2H^+. We note that P_2H^+ is isovalent with Si_2H_2; it also contains two heavy atoms of the second long row (in the periodic table of elements). For Si_2H_2 a bridged structure has been predicted by various authors.[17]

(14) Lee, J.-G.; Cowley, A. H.; Boggs, J. E. *Inorg. Chim. Acta* **1983**, *77*, L61.
(15) Mulliken, R. S. *J. Chim. Phys. Phys.-Chim. Biol.* **1949**, *46*, 491, 615. See also: Kutzelnigg, W. *Einführung in die Theoretische Chemie*; Verlag Chemie: Weinheim/Bergstrasse, FRG, 1978; Vol. 2.
(16) Huheey, J. E. *Inorganic Chemistry*, Harper International SI ed.; Harper and Row: New York, 1983.
(17) Köhler, H. J.; Lischka, H. *J. Am. Chem. Soc.* **1982**, *104*, 5884. Binkley, J. S. *J. Am. Chem. Soc.* **1984**, *106*, 603. Snyder, L. C.; Wassermann, Z. R.; Moskowitz, J. W. *Int. J. Quantum Chem.* **1982**, *21*, 565. Kawai, F.; Noro, T.; Murakami, A.; Ohno, K. *Chem. Phys. Lett.* **1982**, *92*, 479. For the related isoelectronic HSiP see: Dykema, K. J.; Truong, T. N.; Gordon, M. S. *J. Am. Chem. Soc.* **1985**, *107*, 4535. For previous consideration on $[P_2H]^+$ see also: Nguyen, M. T.; Fitzpatrick, N. J. *Chem. Phys. Lett.* **1988**, *146*, 524.

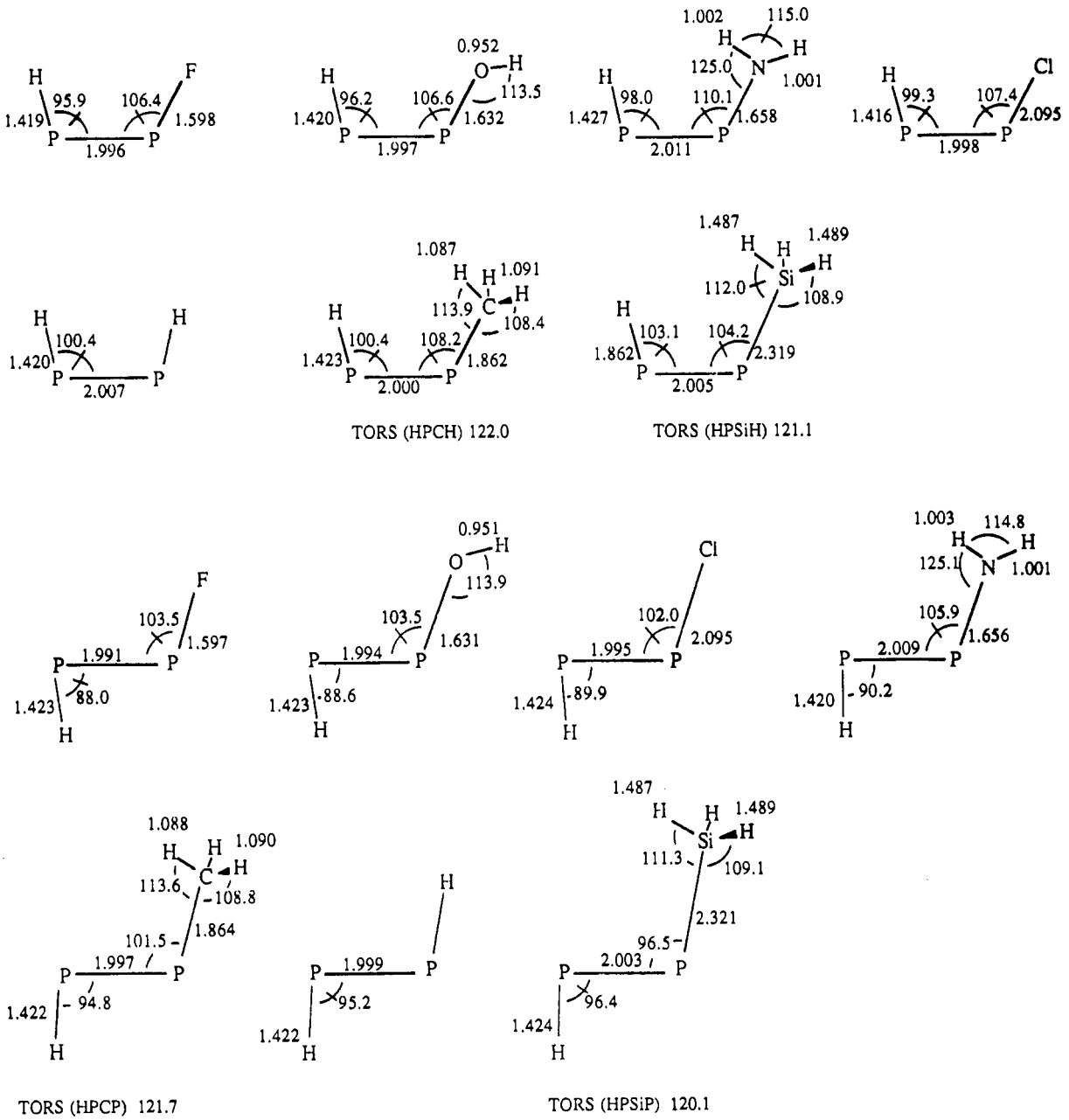

Figure 1. Bonding parameters for the model geometries of diphosphenes (bond lengths in ppm and bond angles in deg).

An important aspect may be viewed here in order to get a deeper understanding of the stability of these unusual structures. In the higher main-group elements (e.g. P, Si, etc.) the valence s orbital is more strongly contracted than the corresponding p orbitals.[18] It is witnessed in some important chemical phemomena as well, e.g. the occupancy of an oxidation state 2 units below the group valence ("inert pair effect"[19]). Consequently, the valence s and p orbitals differ in space extension and overlap less to form strong hybrid orbitals.[18c] Contrary to the case of carbon, the orbitals perfectly match for the formation of hybrid orbitals.

In our recently derived model of orbital nonhybridization,[20] we simulate the effect of s valence orbital contraction in bonding between higher main-group elements qualitatively by comparing energy values for the various structures, obtained from two models at an extended Hückel level: model A, equal Slater exponents for the valence orbitals ($\zeta_{3s} = \zeta_{3p}$); model B, strong contraction of the valence s orbital ($\zeta_{3s} = \zeta_{3p} + 1.0$). Consequently, model A refers to the case of "perfect" isovalent hybridization, while model B mimics the effect of the "inert" s orbital. It results in (i) lone pairs with higher s character and (ii) mixing in of low-lying antibonding orbitals into bonding ones, causing a possible change in molecular structure via second-order Jahn–Teller distortion.

For the case at hand cyclo-P_2H^+ (C_{2v}) and (umbrella-shaped) FPPH may be compared with linear P_2H^+ ($C_{\infty v}$). Assuming SCF-optimized geometries, the former structures (cyclo-P_2H^+, *trans*-FPPH) are stabilized (E(model B) $-E$(model A) = −1.1 and −2.1 eV, respectively), while linear P_2H^+ is raised in energy by +0.5 eV. Although this model is simplified, it provides an understanding for the stabilities of bridged and umbrella-shaped structures as a consequence of "less perfect" hybridization.

At this stage we may summarize our findings as follows: (1) P_2H^+ definitely prefers a bridged structure in which a nonclassical three-center bond between the hydrogen and the two phosphorus atom exists. (2) In the case of the diphosphenes substituted by one electronegative group (atom), e.g. fluorine, a strong charge

(18) (a) This is witnessed in the refined rules for the choice of orbital exponents of a Slater-type wave function: Clementi, E.; Raimondi, D. L. *J. Chem. Phys.* **1963**, *38*, 2686. Burns, C. *J. Chem. Phys.* **1964**, *41*, 1521. (b) For further interpretations of the valence s-orbital contraction see: Pykkö, P.; Desclaux, J.-P. *Acc. Chem. Res.* **1979**, *12*, 276. (c) Its consequence on hybridization has been lucidly discussed: Kutzelnigg, W. *Angew. Chem., Int. Ed. Engl.* **1984**, *23*, 272.

(19) E.g.: Cotton, F. A.; Wilkinson, G. *Advanced Inorganic Chemistry*; Wiley: New York, 1980.

(20) Schoeller, W. W.; Dabisch, T. *Inorg. Chem.* **1987**, *26*, 1081, Schoeller, W. W.; Dabisch, T.; Busch, T. *Inorg. Chem.* **1987**, *26*, 4383.

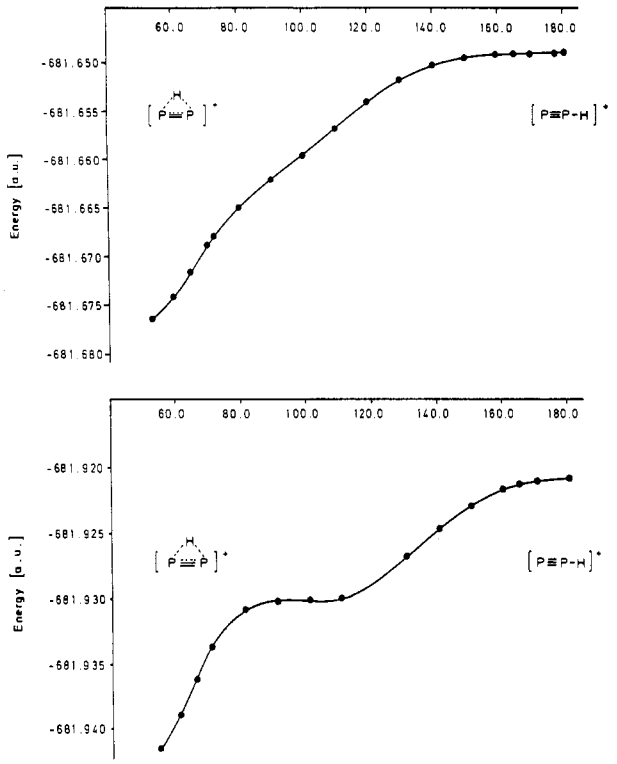

Figure 2. Potential hypersurface of P_2H^+ as a function of valence angle PPH: (top) SCF level; (bottom) SCF/CEPA-1 level.

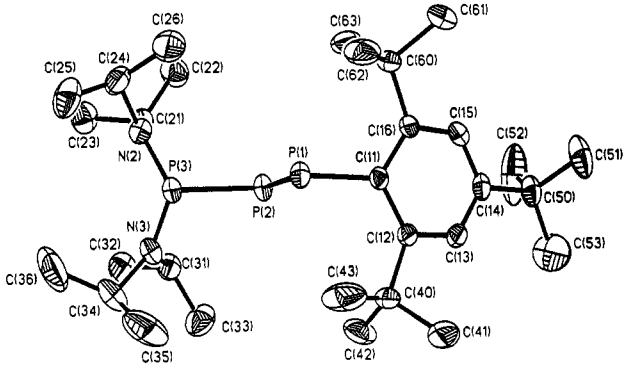

Figure 3. Structure of **8a**.

separation appears. As revealed for the case of FPPH, it refers to a close ion pair of F^- with P_2H^+. Thus, it is logical to expect the tendency for a decrease of the corresponding valence angle and the atom P^β becomes umbrella-shaped. (3) The unusual structures are stabilized by a contraction of the valence 3s orbitals.

For the case at hand, diphosphenes substituted by electronegative groups, an experimental verification has not been reported so far. This will be the subject of the following experimental part of our publication. An experimental verification must rely on structures that are electronically related to this model system. For this purpose we have chosen the diaminophosphino group as a ligand, replacing R^2 by H. It (a) forms very stable cations[21] and (b) allows the recording of a possible through-space interaction via the P_AP_C NMR coupling constant.

c. Structural Studies. The structures of compounds **8a,d,f** are illustrated in Figures 3–5. Selected bond lengths and angles for these compounds are given in Tables VII and VIII. The P(2)–P(3) bond distances (2.23–2.24 Å) are indicative of a bond order of unity, while the P(1)–P(2) bond lengths (2.01–2.03 Å) are similar to those found for diphosphenes.[2]

(21) Cowley, A. H.; Kemp, R. A. *Chem. Rev.* **1985**, *85*, 367.
(22) The structure of **9b** was unambiguously proven by an X-ray analysis: Nieger, M. Doctoral thesis, Bonn, FRG, 1989.

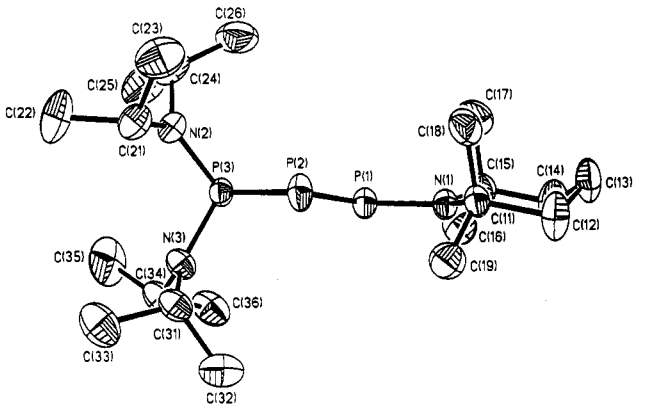

Figure 4. Structure of **8d**.

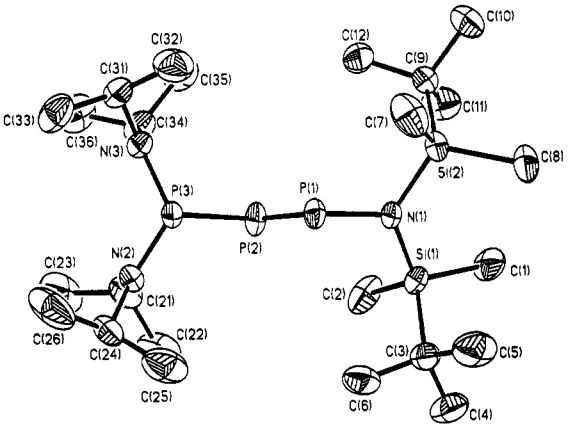

Figure 5. Structure of **8f**.

Table VII. Selected Bond Lengths (Å) and Angles (deg)

	8d	8f	8a
P(1)–P(2)	2.029 (2)	2.011 (2)	2.018 (1)
P(2)–P(3)	2.233 (2)	2.228 (1)	2.242 (1)
P(1)–X[a]	1.691 (4)	1.736 (2)	1.859 (2)
P(3)–N(2)	1.707 (3)	1.687 (3)	1.688 (2)
P(3)–N(3)	1.690 (4)	1.688 (3)	1.692 (2)
X[a]–P(1)–P(2)	114.8 (1)	110.5 (1)	101.2 (1)
P(1)–P(2)–P(3)	89.4 (1)	89.8 (<0.1)	92.3 (<0.1)
P(2)–P(3)–N(2)	100.5 (1)	100.9 (1)	104.5 (1)
P(2)–P(3)–N(3)	101.8 (1)	100.1 (1)	98.4 (1)
N(2)–P(3)–N(3)	107.9 (2)	110.5 (2)	109.0 (1)

[a] **8d,f**, X = N(1); **8a**, X = C(11).

Table VIII. Selected Torsion Angles (deg)

Compound **8d**	
P(2)–P(1)–N(1)–C(11)	2.4 (4)
P(2)–P(1)–N(1)–C(15)	−160.0 (3)
N(1)–P(1)–P(2)–P(3)	177.7 (2)
Compound **8f**	
P(2)–P(1)–N(1)–Si(1)	−60.5 (2)
P(2)–P(1)–N(1)–Si(2)	126.2 (1)
N(1)–P(1)–P(2)–P(3)	−179.8 (1)
Compound **8a**	
P(2)–P(1)–C(11)–C(12)	−83.6 (2)
P(2)–P(1)–C(11)–C(16)	90.8 (2)
C(11)–P(1)–P(2)–P(3)	175.3 (1)

The ligand R adopts in **8a** a nearly orthogonal conformation (angle between the normals to the C(11)–C(16) and P(3)P(2)P(1) planes is 86.6°). This conformation is also preferred in the case of **8f** (Si(1)N(1)Si(2)P(2)–P(3)P(2)P(1)N(1) = 56.7°), while **8d** adopts an almost coplanar conformation (C(11)P(1)N(1)C(15)–P(3)P(2)P(1)N(1) = 12.7°).

In the resulting four-π-electron system the P(1)–N(1) bond in **8d** is significantly shorter (1.67 Å) than in **8f** (1.74 Å). The

Table IX. ^{31}P NMR Data[a] for Phosphino-Diphosphanes $(^iPr_2N)_2P_A-P_B=P_C-R$ (**8a-g**)

R	$\delta(^{31}P)$, ppm			J_{PP}, Hz		
	P_A	P_B	P_C	P_AP_B	P_BP_C	P_AP_C
Mes*	70.4	502.7	554.0	181	574	403
$^iPr_2N$	61.7	245.7	483.9	197	534	541
$Me_3Si_2N(Me_3Si)N$	60.8	298.7	522.3	186	522	505
$(-Me_2C(CH_2)_3CMe_2-)N$	73.7	320.1	496.5	205	574	603
Mes*(H)N	61.4	407.4	544.0	174	570	609
$(Me_2Bu^tSi)_2N$	67.9	442.9	577.6	190	602	566
Mes*O	53.9	386.2	590.2	169	564	601

[a] All values are given relative to H_3PO_4. Positive values designate downfield chemical shifts.

opposite is observed for the PP double-bond lengths (2.03 Å, **8d**; 2.01 Å, **8f**). The bond lengths and bond angles for the $P(N^iPr_2)_2$ ligand are quite normal. However, in the phosphino-diphosphenes the P(1)-P(2)-P(3) angle is smaller; it even decreases in the series **8a** > **8f** > **8d** below 90°!

d. NMR Studies. The ^{31}P NMR data for compounds **8a-g** are given in Table IX. All compounds give 12 lines according to an AMX pattern (three doublets of doublets). The resonances at high fields (δ 54-74 ppm) are due to the phosphino group while those at lower fields are indicative of the PP double-bond system.[1a] Note that the shift at the nucleus P_B shows a significant correlation with the "nature" of the ligand R. It can be interpreted in terms of the π-donating ability of the ligand. In the series of the amino-substituted derivatives **8b-g** the signal is shifted from 443 ppm for **8f** (with an almost orthogonal arrangement of the NSi_2 group with respect to the central π system) to 246 ppm for **8b**, which adopts a coplanar conformation. In the case of **8d** (δ 320 ppm) the nitrogen ligand is twisted by 12° out of the NPP plane. A similar trend in $\delta(^{31}P)$ is observed for the nucleus P_A, but to a smaller extent. The values for the $^1J_{P(B)P(C)}$ coupling constant (534-602 Hz) are similar to those observed for asymmetric substituted diphosphenes. However, the most remarkable features of all phosphino-diphosphenes are the large two-bond coupling constants $^2J_{P(A)P(C)}$ (400-600 Hz), which are in some cases larger than the values found for the interaction of the double-bond system in the same molecule (**8b,d,e,g**).

As has been shown by X-ray data analysis for **8a,d,f**, the two phosphorus lone pairs are nearly in the same plane. This special conformation combined with the small angle $P_aP_BP_C$ involves enhancement of $^2J_{P(B)P(C)}$.

Conclusions

The results of our investigations can be summarized as follows.

(1) According to quantum-chemical calculations an electronegative substituent at the PP double bond causes the formation of the close ion pair X^-PPH^+. Concomitantly, unusual structures are predicted that depart from the conventional picture of known double-bond systems. The β-phosphorus atom tends to adopt an umbrella conformation, i.e. a bridged structure.

(2) The theoretical predictions are fully confirmed by structural investigations on a selected variety of substituted diaminophosphino-diphosphenes, which were synthesized for this purpose. These structures are the first ones toward a realization of bridged structures in the chemistry of multiple bonding between heavier main-group elements.

Acknowledgment. This work was supported by the Deutsche Forschungsgemeinschaft and the Fonds der Chemischen Industrie. The calculations were performed on a Cyber 205 computer (Ruhr-Universität Bochum). We thank Udo Welz for computational assistance.

Registry No. *cis*-**1** (R^α = H, R^β = H), 87678-58-8; *trans*-**1** (R^α = H, R^β = H), 87678-57-7; *cis*-**1** (R^α = F, R^β = H), 122049-31-4; *trans*-**1** (R^α = F, R^β = H), 122049-48-3; *cis*-**1** (R^α = Cl, R^β = H), 122049-32-5; *trans*-**1** (R^α = Cl, R^β = H), 122049-49-4; *cis*-**1** (R^α = OH, R^β = H), 122049-33-6; *trans*-**1** (R^α = OH, R^β = H), 122049-50-7; *cis*-**1** (R^α = NH_2, R^β = H), 122049-41-6; *trans*-**1** (R^α = NH_2, R^β = H), 122049-51-8; *cis*-**1** (R^α = CH_3, R^β = H), 122049-42-7; *trans*-**1** (R^α = CH_3, R^β = H), 122049-52-9; *cis*-**1** (R^α = SiH_3, R^β = H), 122049-43-8; *trans*-**1** (R^α = SiH_3, R^β = H), 122049-53-0; **2**, 117270-09-4; **3**, 91443-42-4; **5**, 54043-94-6; **6c**, 111437-98-0; **6d**, 64945-24-0; **6e**, 122049-47-2; **6f**, 85909-11-1; **6g**, 796-62-3; **8a**, 122049-34-7; **8b**, 122049-35-8; **8c**, 122049-36-9; **8d**, 122049-37-0; **8e**, 122049-38-1; **8f**, 122049-39-2; **8g**, 122049-40-5; **9b**, 122049-45-0; $(i\text{-}Pr_2N)_2PP(Cl)P(SiMe_3)Mes^*$, 122049-30-3; P_2H^+ (cyclic), 122049-44-9; $(i\text{-}Pr_2N)_2PP(Li)SiMe_3$, 122049-46-1; P_2H^+ (linear), 12339-20-7.

Contribution from the Institut für Physikalische und Theoretische Chemie, Universität Tübingen, 7400 Tübingen, West Germany, and Department of Chemistry, Clemson University, Clemson, South Carolina 29634-1905

Molecular Structure and Internal Rotation Potential of Perfluoro-2,3-diaza-1,3-butadiene, $CF_2=N-N=CF_2$. An Electron Diffraction and ab Initio Study

Heinz Oberhammer,*[,†] Charles W. Bauknight, Jr.,[‡] and Darryl D. DesMarteau[‡]

Received May 5, 1989

A gas-phase electron diffraction study of perfluoro-2,3-diaza-1,3-butadiene results in a planar trans structure with the following geometric parameters (r_a values with 3σ uncertainties): N-N = 1.421 (12), C=N = 1.264 (7), C-F = 1.304 (4) Å; N-N=C = 112.7 (9), F-C-F = 110.8 (9)°. The CF_2 groups are tilted by 5.0 (8)° toward the nitrogen lone pairs. No additional conformer has been observed. Ab initio calculations for $CH_2=N-N=CH_2$ (6-31G** basis) and $CF_2=N-N=CF_2$ (6-31G* basis) demonstrate that the internal rotation potentials change drastically if electron correlation is included at the MP2 level. Whereas SCF-HF calculations predict the planar trans forms to be the only stable conformers, the MP2 method predicts additional high-energy gauche conformers with ΔE = 0.8 ($CH_2=N-N=CH_2$) and 1.8 kcal mol^{-1} ($CF_2=N-N=CF_2$). Both values are in good agreement with experiment, ΔE = 1.2 (5) kcal mol^{-1} for the parent compound and $\Delta G \geq$ 1.8 kcal mol^{-1} for the fluorinated species.

Introduction

Structure and conformational properties of the simplest conjugated systems, 1,3-butadiene and the isoelectronic glyoxal, have attracted considerable interest over the past decades. It is well established by experimental methods (electron diffraction,[1] vibrational spectroscopy[2]) and by ab initio calculations[3,4] that the

† Universität Tübingen.
‡ Clemson University.

(1) Kveseth, K.; Seip, R.; Kohl, D. A. *Acta Chem. Scand. Ser. A* **1980**, *34*, 31.
(2) Carreira, L. A. *J. Chem. Phys.* **1975**, *62*, 3851. Panchenko, Yu. N.; Csaszar, P. *J. Mol. Struct.* **1985**, *130*, 207.

0020-1669/89/1328-4340$01.50/0